Multitechnique characterization of conventional and experimental Ag-based brazing alloys for orthodontic applications

Ntasi, Argyro ; Al Jabbari, Youssef S ; Silikas, Nick ; Eliades, Theodore ; Zinelis, Spiros

Abstract: OBJECTIVES To characterize the microstructure, mechanical properties, ionic release and tarnish resistance of conventional and experimental Ag-based soldering alloys for orthodontic applications. METHODS Disk shaped specimens were prepared from four commercial Ag based soldering alloys [Dentaurum Universal Silver Solder (DEN), Orthodontic Solders (LEO), Ortho Dental Universal Solder (NOB), and Silver Solder (ORT)] and four experimental alloys Ag12Ga, Ag10Ga5Sn, Ag20In and Ag7Sn. The elemental composition and microstructure was determined by SEM/EDX and XRD analysis, while the mechanical properties were determined by Instrumented Indentation Testing. Ionic release of Ag, Cu, Zn, Ga, In and Sn was determined by ICP-EAS in 0.9% NaCl and Ringer's solutions after 28, 49 and 70 days. Tarnish resistance was also tested and colorimetry was applied to quantify the differences in color (DE) before and after immersion in testing media. DSC was used to determine the melting range of the experimental alloys. Mechanical properties, ionic release and DE were statistically compared by ANOVA and Holm-Sidak multiple comparison test (a=0.05). RESULTS All commercially alloys belong to the Ag-Zn-Cu ternary system and consist a Ag rich face centered cubic (FCC) and Cu (FCC) phase. The former is the predominant phase also in experimental alloys. Conventional alloys demonstrated higherhardness, less ductility and lower melting rangers compared to experimental alloys. Immersion testing revealed the release of Cu and Zn ions from the commercially alloys and Ga ions from AgGa and AgGaSn while no ionic release was identified for AgIn and AgSn. All alloys failed tarnish testing according to ISO 10271 showing DE values much higher than the clinical acceptable limit (3.7). SIGNIFICANCE The conventional Ag based soldering alloys showed substantial differences in their microstructure, mechanical properties and ionic release, and thus different clinical performance is anticipated. Ga, Sn and In might be employed as alloying addition to modify the properties of Ag brazing alloys.

DOI: https://doi.org/10.1016/j.dental.2018.01.003

Materials, 34(3):e25-e35.
DOI: https://doi.org/10.1016/j.dental.2018.01.003

Multitechnique characterization of conventional and experimental Ag-based brazing alloys for orthodontic applications.

Ntasi A, Al Jabbari YS, Silikas N, Eliades T, Zinelis S.

Dent Mater.2018 Mar;34(3):e25-e35. doi: 10.1016/j.dental.2018.01.003.

Abstract.

Objectives. To characterize the microstructure, mechanical properties, ionic release and tarnish resistance of conventional and experimental Ag-based soldering alloys for orthodontic applications.

Methods. Disk shaped specimens were prepared from four commercial Ag based soldering alloys [Dentaurum Universal Silver Solder (DEN), Orthodontic Solders (LEO), Ortho Dental Universal Solder (NOB), and Silver Solder (ORT)] and four experimental alloys Ag12Ga, Ag10Ga5Sn, Ag20In and Ag7Sn. The elemental composition and microstructure was determined by SEM/EDX and XRD analysis, while the mechanical properties were determined by Instrumented Indentation Testing. Ionic release of Ag, Cu, Zn, Ga, In and Sn was determined by ICP-EAS in 0.9% NaCl and Ringer's solutions after 28, 49 and 70 days. Tarnish resistance was also tested and colorimetry was applied to quantify the differences in color (DE) before and after immersion in testing media. DSC was used to determine the melting range of the experimental alloys. Mechanical properties, ionic release and DE were statistically compared by ANOVA and Holm-Sidak multiple comparison test (a= 0.05).

Results. All commercially alloys belong to the Ag-Zn-Cu ternary system and consist a Ag rich face centered cubic (FCC) and Cu (FCC) phase. The former is the predominant phase also in experimental alloys. Conventional alloys demonstrated higherhardness, less ductility and lower melting rangers compared to experimental alloys. Immersion testing revealed the release of Cu and Zn ions from the commercially alloys and Ga ions from AgGa and AgGaSn while no ionic release was

identified for AgIn and AgSn. All alloys failed tarnish testing according to ISO 10271 showing DE values much higher than the clinical acceptable limit (3.7). **Significance.** The conventional Ag based soldering alloys showed substantial differences in their microstructure, mechanical properties and ionic release, and thus different clinical performance is anticipated. Ga, Sn and In might be employed as alloying addition to modify the properties of Ag brazing alloys.

Keywords: Ag-brazing alloys, SEM/EDX, XRD, ICP-AES, DSC, Mechanical properties, Tarnish resistance, Colorimetry.

1. Introduction

Brazing of dissimilar stainless steel (SS) alloys (i.e orthodontic wires and bands) is mandatory in the manufacturing of orthodontic appliances such as headgears, space maintainers, brackets, hyrax appliances and others. [1-3]. Despite their extensive use in these orthodontics devices, the release of metallic toxic ions from them due to corrosion or wear mechanisms[4] is a constant concern of modern dental literature[5, 6].

All contemporary Ag based brazing alloys belong to the Ag-Cu-Zn ternary system [7] and many in vitro studies have found out that this ternary system is vulnerable to Cu and Zn release [8-12] and coupling with SS alloys may trigger galvanic action[13]. Indeed a previous study reported that the potential difference between SS and Ag brazing alloys is almost double the threshold for galvanic corrosion[9]. Experimental findings were recently confirmed by two different studies based on clinical data. Measuring the concentration of metallic ions in human saliva up to 60 days after the placement of Hyrax appliances, Freitas et al., [1] reported the release of Cu, Zn and Cd from Ag brazing alloys. In an other study, the intraoral decomposition of two commercially available Ag brazing alloys were proven by comparing their elemental composition before and after intraoral aging [3].

The clinical implications of these findings are twofold. The decomposition of Ag brazing alloys has been associated with the mechanical degradation of the joint itself and thus with the early failure of orthodontic devices, especially of space maintainers [14-19]. In this scenario the failed appliance is replaced by a new one, increasing the uptake of released elements[3]. The uptake of Cu and Zn by the human body is associated with different biological consequences. The intake of Cu beyond the acceptable oral limit [20] is associated with liver and gastrointestinal

complications [21] and atherogenesis [22], while it may trigger oxidative damage and carcinogenesis and neurodegenerating processes [21, 23-26] through a mechanism forming reactive oxygen species (ROS). The excess intake of Zn has been proven to be cytotoxic for fibroblasts [27] and it has also been implicated in reduced HDL cholesterol and immunological response [28]. In addition beyond the adverse effect of diffusion of Cu and Zn in the body the accumulation of these elements at the adjacent tissues has been associated with allergic reaction[29] and oral lesions[30]. In any case the decomposition of a biomaterial in the oral cavity is far beyond the ideal.

In order to overcome the aforementioned limitations new formulations of Ag brazing alloys without Cu and Zn should be developed and thus the aim of this study was the comparative analysis of conventional and experimental alloys. The null hypothesis was that experimental alloys will show better properties than conventional ones.

2. Materials and Methods

2.1 Specimen preparation

Four commercially available Ag brazing alloys for the manufacturing of space maintainers and four experimental alloys were tested. The four experimental alloys were prepared in an induction melting machine (Ducatron S3, UGIN' Dentaire, Seyssins, France) by melting pre-weighted quantities in a silicate crucible (UGIN' Dentaire) appropriate for melting precious metal alloys. The pre-weighted quantities were inductively melted and left to cool to ambient temperature in the silicate crucible. For the preparation of the alloys the following pure elements were used: Ag 99.99 wt% (AG006105/4, Goodfellow, Huntingdon, England), Ga 99.99 wt% (S97020, Johnson Matthey GmbH, Karlsruhe, Germany), Sn 99.995 wt% (SN006102/4, Goodfellow) and In 99.99 wt% (9300, Johnson Matthey GmbH). Table

1 shows the elemental composition, the melting range of the commercial alloys according to their manufacturers and the code used for them in this study. Also shown the experimental alloy compositions.

All commercial alloys are provided as wires to facilitate the brazing procedure. A small quantity of each commercial alloy was melted in a reducing flame and left to solidify in a circular mould. Eighteen disk shaped samples (approximately 6 mm in diameter and 2mm in heigth) were prepared from each experimental alloy. The wires of NOB and DEN contain the requested flux as a separated layer in the wire structure, while for LEO and ORT the corresponding fluxes from their manufacturers were used (Leone fluoride flux paste (Leone S.p.a, Italy), and Ortho Technology TruFlow Orthodontic Flux (Ortho Technology) respectively). One sample from each group was kept as cast and the rest were embedded in an epoxy resin (Caldofix, Struers, Ballerup, Denmark). Afterwards the specimens of all groups were ground through 4000 grit silicon carbide paper under water cooling and polished with 1μm diamond suspension (DiaPro suspension solution, Struers) in a grinding/polishing machine (Dap-V, Struers). Finally the samples were cleaned in an ultra sonic bath with ethanol for 3 minutes and then rinsed with water and dried.

2.2 Differential Scanning Calorimetry (DSC).

The melting temperature range of the experimental alloys was determined by DSC analysis using a differential photo calorimeter analyzer (STA 449 C, NETZSCH, Selb, Germany) equipped with a UV 5000 lamp. The measurements were preformed in a temperature range from 22 to 1000 ^{o}C and with a heating rate of 10 ^{o}C/min. Solidus and liquidus temperatures were defined at the points of first and last deviations from the baseline respectively.

2.3 Scanning Electron Microscopy / X-ray Energy Dispersive Spectroscopy (SEM/EDX) analysis

Three specimens from each group were imaged employing scanning electron microscopy (SEM) (Quanta 200, FEI, Hillsboro, OR, USA). Mean atomic contrast backscattered electron images (BEI) were taken using a solid state detector (SDD) under high vacuum (10^{-6} mbar), 30 keV accelerating voltage, 96μA beam current and 1000X nominal magnification.

The elemental compositions of both experimental and commercial alloys were analyzed by energy-dispersive X-ray microanalysis (EDX), using an X Flash 6|10 Silicon Drift Detector (SDD; Bruker, Berlin, Germany). Two spectra from each specimen were collected employing area scan mode (130μm×130μm sampling area) under the aforementioned conditions with a 200-second acquisition time and 1% detector dead time. Indicative elemental compositions of different phases based on mean atomic number contrast were recorded by spot analysis. The quantitative analysis was carried out by ESPRIT ver 1.9 software (Bruker) under a nonstandard mode, using ZAF (atomic number, absorbance, fluorescence) correction methods. The quantitative results from area and spot analysis were averaged.

2.4 X-ray Diffraction (XRD) analysis

The specimens were subjected to XRD analysis (D8 Advance, Bruker, Massachusetts, USA) using CuKa radiation, 40 KV accelerating voltage, 40 mA beam current, 30^{o} – 110^{o} 2θ angle scan range, 0.02^{o}/s scanning speed, 0.02^{o} sampling pitch and 1 s preset time.

2.5 Instrumented Indentation Testing (IIT).

The mechanical properties of all groups were identified employing IIT. Five specimens from each group were analyzed by a universal hardness testing device ZHU0.2/Z2.5 (Zwick Roell, Ulm, Germany). Three force-indentation depth curves were recorded for each specimen using 29.4 N maximum load, 2-second dwell time and a Vickers indenter. The mean values of selected properties were used to characterize each specimen . Based on the aforementioned curves the Martens Hardness (HM), the indentation modulus (E_{IT}) and the elastic index η_{IT} were calculated according to ISO 14577-1[31].

2.6 Ionic release.

In order to evaluate the ionic release of metal ions from the alloys tested the specimens were immersion testedin two solutions. All tests were performed in the same tubes with caps and electrolyte solutions of either 0.9% NaCl or Ringer's solution (9g NaCl, 0.24g $CaCl_2 \cdot 6H_2O$, 0.43g KCl, 0.2g $NaHCO_3$ in 1000ml distilled water). The tubes were filled with solution and sealed to prevent evaporation. Eight specimens from each material were used. Four of them were tested in NaCl and the other four in Ringer's solution. A small amount of solution (2 ml) was taken from each tube after 28, 49 and 70 days. After immersion the specimens were studied under a stereomicroscope (STM-Olympus Optical CO Ltd, Tokyo, Japan) and images were obtained. Then the solutions were analyzed for Ag, Cu, Zn, Sn, Ni, Ga and In, using Inductive Coupled Plasma Atomic Emission Spectroscopy (ICP-AES) with a Perkin Elmer Optima 3000 ICP-AES spectrometer under 1.5ml/min flow rate and 10-20 s read time.

2.7 Tarnish resistance

Six specimens from each group were tested for tarnish resistance according to ISO 10271[32]. A freshly made test solution was prepared by dissolving 3.1g of $Na_2S \times 9H_2O$ in 1000 ml of water and five specimens were immersed in it for 72h. The sixth specimen was used as control. The borosilicate glasses and specimens were kept in an oven at 37 ^oC. The treated specimens were visually compared with the untreated one and any surface deterioration and/or discoloration was recorded. In addition to the ISO requirements the tested specimens were colorimetrically evaluated with a colorimeter (Microcolor, Data Station, DrLange, Braive Instruments, Leige, Belgium) according to the CIE Lab (Commision Internationale de l'Eclairage, L, a, b) system. Each specimen was measured before and after immersion and the color difference (DE) was determined according the following equation:

$$DE=[(L_1-L_2)^2+(a_1-a_2)^2+(b_1-b_2)^2]^{1/2}$$

The L parameter is positive and represents brightness while a and b coordinates indicated the positions on the red - green and yellow - blue axes respectively.

2.8 Statistical analysis

The results of mechanical property (HM, E_{IT}, and η_{IT}) and DE tests were statistically compared using One Way Analysis of Variance (ANOVA) employing material as the discriminating variable. The results of ionic release were statistically compared by 2 way ANOVA using material and immersion time as independent variables. In both cases a pairwise multiple comparison (Holm-Sidak) test at 95% level of significance (a=0.05) was used to allocated significant differences among groups.

3. RESULTS

3.1 Differential Scanning Calorimetry (DSC)

Figure 1 presents DSC thermograms from the four experimental alloys tested. AgGa exhibits two poorly resolved peaks between 392 and 436^{o}C, a sharp peak at higher temperatures (600-618 ^{o}C) and a broad peak between 639 and 789 ^{o}C. AgGaSn has a sharp peak at 618-633 ^{o}C range and a broad peak at 640-793 ^{o}C. AgIn and AgSn show single endothermic peaks in the ranges of 688-832 ^{o}C and 830-927 ^{o}C, respectively. AgGa exhibited the lowest melting temperature, followed by AgGaSn, AgIn and AgSn. Contrary to the other alloys AgGa exhibited an oxidation/decomposition peak after melting (1D)

3.2 SEM/EDX analysis

Figure 2 presents the BEI of all alloys tested at 1000X nominal magnification. The locations in different phases, indentified by different mean atomic number contrast, where spot analysis was performed are pointed out on the images with an asterisk. The DEN and NOB microstructures (Fig 2A, C) contain dendrites and needle like formations within a matrix of a lower mean atomic number a formation probably originated from a eutectic reaction. LEO (Fig 2B) exhibits a lower mean atomic number phase dispersed in a high atomic number contrast matrix. ORT (Fig 2D) illustrates the distribution of a lower mean atomic number phase in a higher mean atomic number phase. Matrix of ORT depicts medium mean atomic number contrast compared to aforementioned phases. AgGa and AgGaSn microstructure consists of two mean atomic number contrast phases (Fig 2E and F) while no mean atomic number contrast where identified for AgIn and AgSn (Fig.2G and H). On Table 2 the results of the area and spot EDX analysis are illustrated. DEN and NOB have higher Ag content compared to LEO and ORT. The former contains Sn whereas the latter

Ni. The EDX spot analysis revealed that DEN and NOB share similar elemental compositions in L and H different mean atomic number phases with the H areas enriched in Ag content and depleted in Cu and Zn. In LEO and ORT, Ag content decreases from H towards L while Cu and Zn follows the inverse trend. Despite the differences in their elemental compositions all the aforementioned phases are characterized as Ag based phase apart from L of LEO and ORT which is a Cu based phase. Both phases in AgGa and AgGaSn are Ag based with the L phase having lower Ag content and being enriched in Ga and Sn (with Sn only in the case of AgGaSn alloy).

3.3 X-ray Diffraction (XRD) analysis

From the XRD analysis of the commercially alloys tested (Fig. 3) derives that they all have the same Ag based face centered cubic (FCC) and Cu based facr centered cubic (FCC) phases. One additional phase, the CuZn BCC β phase was identified for ORT. AgGa, AgGaSn and AgSn contain an FCC Ag phase and intermetallic phases that are noted on the spectra of the XRD analysis (Fig.3).

3.4 Instrumented Indentation Testing (IIT).

Fig 4 illustrates representative force-indentation depth curves for all materials tested. The curves with deeper indentation depths denote softer materials. All mechanical properties tested are presented in Table 3. No significant differences were identified among commercial alloys, while all experimental alloys have significantly lower HM. AgGa showed the highest HM among experimental alloys with statistically significant differences compared to AgIn and AgSn. LEO and ORT showed higher E_{IT} compared to DEN and NOB. All experimental alloys showed decreased E_{IT}

without difference among them. Significant differences were also identified in (η_{IT}) elastic index among materials tested.

3.5. Ionic release

ICP results revealed that all commercially alloys released Cu and Zn during immersion whereas AgGa and AgGaSn released Ga (Fig 5 and 6) in both solutions tested. Ag, In and Sn were not identified in all solution tested.

Statistical analysis revealed no significant differences for Cu in Ringers solution between NOB and ORT after 70 days, for Zn between LEO and NOB after 28 days, and for NOB between 28 and 49 days (Fig 5).

For NaCl no significant differences were determined for Cu between DEN and LEO after 28 days and LEO and NOB after 70 days. No significant differences were also found for DEN between 28 and 49 days, and for ORT between 49 and 70 days. LEO and NOB did not show significant differences after 28 and 49 days.

In general Cu and Zn did not reveal a uniform behavior, whereas Ga tends to increase over immersion time (Fig 5 and 6).

After immersion testing the commercially alloys show a large amount of color depositions on their surface. In contrast the experimental alloys demonstrated a gross dendritic structure after immersion testing (Fig 7).

3.6 Tarnish resistance

All samples showed visible signs of change in color and surface gloss compare to their reference and thus failed to comply with ISO requirements. Based on colorimetric analysis AgSn and Leo showed the highest DE values while AgGa, AgIn

and AgGaSn showed the lowest. ORT, NOB and ORT demonstrated intermediated values. The results and statistical outcome is appeared in Fig 8.

4. DISCUSSION

Based on the results of this study the null hypothesis must be partially accepted as experimental alloy demonstrated less ionic release, better tarnish resistance but inferior mechanical properties.

In order to overcome the inherent drawback of in vivo decomposition of Ag based brazing alloys [1, 3] new formulations must be developed. However the selected alloying elements should fulfill the following requirements: a) The selected elements should decrease the melting point of Ag as brazing alloys must melt at temperatures lower than the solidus of SS used in custom made orthodontic devices (PH 17-4 SS and AISI 303SS[3]). b) To enhance corrosion resistance, especially in galvanic action, the content of selected elements should not exceed the solubility limit in the solid state in order to provide a single phase material instead of the conventional multiphase ones[7]. c) The selected elements must not have been associated with biocompatibility problems. Taking in account all the aforementioned constrains and the binary phase diagrams of Ag-Ga, Ga-Sn, Ag-In and Ag-Sn [33-36] the four experimental formulations were produced.

EDX results (Table 2) showed that all commercially alloys belong to Ag-Cu-Zn system. LEO and ORT also contain small quantities of Sn and Ni, respectively, to decrease their melting points[37]. Both alloys have increased Cu content compared to DEN and NOB justifying their lower melting points. All experimental alloys demonstrated higher liquidus. The AgSn and AgIn alloys exhibited single peaks for their melting ranges and higher liquidus temperatures then AgGa and AgGaSn alloys.

AgGa also exhibited a peak at low temperatures (392-436 ^{o}C) which is actually consists of two peaks. Tha small peak at 392 ^{o}C results from eutectoid reaction while the larger peak at 436 ^{o}C is associated with the diffusionless solid state transformation ζ⇔ ζ′ (ζ and ζ′ stand for a 30% at Ga phases with ζ and ζ' appeared above and below 440 ^{o}C respectively)[38].

DEN and NOB share similar microstructure as revealed by BEI (Fig 2 A and C). The primary dendrites of Ag rich solid solution phase (Ag-FCC) are formed first during solidification according to the Ag-Cu-Zn ternary phase diagram [39] followed by the transformation of the remaining liquid to acicular (Ag FCC) and Cu rich solid solution phases (Cu FCC) at lower temperatures. Both phases have been identified by XRD analysis (Fig 3) and are in accordance with previous studies[37]. Despite their similarity in their formulations LEO and ORT showed different microstructures (Fig 2). LEO exhibited two Ag based phases (Table 2) and one Cu rich phase. The former should be matched to Ag-FCC and the latter to a-CuZn phase according to XRD spectrum. ORT depicted some primary dendrites probably of Cu rich FCC solid solution (low atomic number) in a matrix of eutectic.. Beyond Ag-FCC and a-CuZn XRD revealed also the presence of b-CuZn. The microstructural differences between LEO and ORT verify the significant effect of Sn and Ni in the microstructure of Ag-Cu-Zn according to previous studies[37]. All the identified phases after XRD analysis are in accordance to previously published data of Ag soldering alloys based on Ag-Cu-Zn ternary system [40-46].

AgGa and AgGaSn consist of a high mean atomic number phase which should be appended to Ag-FCC phase which is in accordance with the respective phase diagrams [33, 47] and its presence is verified by the XRD analysis. Additionally the formation of intermetallic compounds is predicted for the Ag-Ga and

Ag-Sn systems [38, 47, 48] and may correspond to the low mean atomic number phases.

The BE images for the AgIn and AgSn demonstrated a single phase according to mean atomic number differences, though the XRD analysis revealed different intermetallic compounds. For AgSn the identification of a Ag base solid solution according to the XRD results, is in accordance with the Ag-Sn phase diagram [47]. Any deviations of the identified phases for the experimental alloys from those found in bibliography may be attributed to rapid cooling during the preparation of the test specimens, which is far off the thermodynamic equilibrium conditions imposed by phase diagrams. However this rapid cooling condition is what happens in every day practice during the manufacturing of brazing orthodontic appliances and thus what it is expected to be placed intraorally. Definitely further research with advanced analytical techniques (such as TEM-EDS, XPS etc.) can provide substantial information for both the full phase characterization of these multi phase alloys and the solidification mechanism.

IIT results showed that all experimental alloys have inferior mechanical properties (HM and E_{IT}) compare to conventional ones (Table 3). All conventional alloys showed equal HM values but LEO and ORT showed higher E_{IT} compared to DEN and NOB indicating that the higher content of Cu in resulted microstructure have a beneficial effect on this property. The lower the elastic index the more ductile the material is and thus ORT are more ductile among the conventional alloys tested in accordance to previous data showing that brazing materials with Cu, Zn and Sn express satisfactory ductility [49, 50]. Based on elastic index (Table 3) the experimental materials are more ductile compared to conventional alloys but they showed significantly lower HM and E_{IT} indicating that the selected alloying elements

have lower strengthening effect compared to Cu and Zn. Lower HM may indicate inferior resistance to wear phenomena while lower elastic modulus may demand thicker joints to withstand the same loading.

The fact that all commercially alloys released Cu and Zn during immersion testing justifies the results of in vivo findings [1, 3]. The release rates of Cu and Zn are surprisingly decreased over time which may be attributed to the consumption of these elements in the formation of multicolor surface layers as shown in Fig 7. Therefore the aforementioned elements are finally retained on the alloy surface decreasing their concentration in solution. The experimental alloys, which contain Ga demonstrate a continuous increase of the released Ga ions over immersion time implying a continuous release process. Given than neither Ag nor Sn were identified, the release of Ga may be appended on a selective dissolution mechanism. This speculation is further strengthened by the higher release of AgGa alloy with higher Ga content compared to AgGaSn. AgIn and AgSn did not release any ions during immersion testing denoting a tenacious resistance to ionic release in the selected reagents.

All alloys failed to tarnish resistance testing according to ISO 10271[32] and color change (DE) were found far above the limit of 3.7 which the differences are clinically visible [51]. This experimental finding fits well with the appearance of silver joints during intraoral aging[3]. AgSn showed the highest DE values where the rest three experimental alloys the lowest. Although there is no data for Ga, In has a beneficial effect on tarnish resistance forming a thin protective layer on the alloy surface [52].

Though, in order to replace the existing commercially alloys with the experimental ones the ability of these alloys to bind together the various parts of the

orthodontic devices the biocompatibility, as well as their flowability after their transformation to wires must be further examined.

Concluding, the experimental alloys produced have very low ionic release but inferior mechanical properties and still other properties must be further tested. However this study can be the springboard for further research on the development of new Cu and Zn free Ag based soldering alloys for orthodontic applications.

Conclusions:

- The conventional Ag based soldering alloys demonstrated substantial differences in their microstructure, mechanical properties and ionic release.
- Ga, In and Sn provided less strengthening effect compared to Cu and Zn
- In and Sn have a more beneficial effect on ionic release compared to Ga.

References

[1]. Freitas MP, Oshima HM, Menezes LM. Release of toxic ions from silver solder used in orthodontics: an in-situ evaluation. Am J Orthod Dentofacial Orthop 2011;140:177-81.

[2]. Zinelis S, Annousaki O, Eliades T, Makou M. Elemental composition of brazing alloys in metallic orthodontic brackets. Angle Orthod 2004;74:394-9.

[3]. Soteriou D, Ntasi A, Papagiannoulis L, Eliades T, Zinelis S. Decomposition of Ag-based soldering alloys used in space maintainers after intra-oral exposure. A retrieval analysis study. Acta Odontol Scand 2012;72:130-38.

[4]. House K, Sernetz F, Dymock D, Sandy JR, Ireland J. Corrosion of Orthodontic appliances-should we care? Am J Orthod Dentofacial Orthop 2008;133:584-92.

[5]. Eliades T., Athanasiou A.E. In vivo aging of Orthodontic Alloys: Implications for Corrosion Potential, Nickel Release, and Biocompatibility. Angle Orthodontist 2002;72:222-37.

[6]. Eliades T., Bourauel C. Intraoral aging of orthodontic materials: The picture we miss and its clinical relevance. Am.J. Orthod. Dentofacial Orthop. 2005;127:403-12.

[7]. Ntasi A, Al Jabbari Y, Mueller WD, Eliades G, Zinelis S. Metallurgical and electrochemical characterization of contemporary silver-based soldering alloys. Angle Orthod 2014;84:508-15.

[8]. Heidemann J, Witt E, Feeg M, Werz R, Pieger K. Orthodontic soldering techniques: aspects of quality assurance in the dental labaratory. J Orofac Orthop 2002;63:325-38.

[9]. Berge M, Gjerdet NR, Erichsen ES. Corrosion of silver soldered orthodontic wires. Acta Odontol Scand 1982;40:75-9.

[10]. Mikulewicz M, Chojnacka K. Release of metal ions from orthodontic appliances by in vitro studies: a systematic literature review. Biol Trace Elem Res 2011;139:241-56.

[11]. Mikulewicz M, Chojnacka K, Wolowiec P. Release of metal ions from fixed orthodontic appliance: an in vitro study in continuous flow system. Angle Orthod 2014;84:140-8.

[12]. Staffolani N, Damiani F, Lilli C, Guerra M, Staffolani NJ, Belcastro S, et al. Ion release from orthodontic appliances. J Dent 1999;27:449-54.

[13]. Vahed A, Lachman N, Knutsen RD. Failure investigation of soldered stainless steel orthodontic appliances exposed to artificial saliva. Dent Mater 2007;23:855-61.

[14]. Tulonuglu O, Ulusu T, Genc Y. An evaluation of survival of space maintainers: A six year follow up study. J Contemp Dent Pr 2005;6:1-8.

[15]. Rajab LD. Clinical performance and survival of space maintainers: evaluation over a period of 5 years. J Dent Child 2002;69:156-60.

[16]. Baroni C, Franchini A, Rimondini L. Survival of different types of space maintainers. J Pediatr Dent 1994;16:360-61.

[17]. Qudeimat MA, Fayle SS. The longevity of space maintainers: A restrospective study. J Pediat Dent 1998;20:267-72.

[18]. Tunk ES, Bayrak S, Tuloglu N, Egilmez T, Isci D. Evaluation of survival of 3 different fixed space maintainers. Pediatr Dent 2012;34:97-102.

[19]. Fathian M, Kennedy DB, Nouri MR. Labaratory-made space maintainers: A 7-year retrospetive study from private pediatric dental practice. Pediatr Dent 2006;29:500-06.
[20]. IPCS. Principles and methods for the assesment of risk frim essential trace elements. Environmental health criteria document. In: Organization WH, editor. Geneva: International Programme on Chemical Safety.; 2002.
[21]. Gaetke LM, Chow CK. Copper toxicity, oxidative stress and antioxidant nutrients. Toxicology 2003;189:147-63.
[22]. Haidari M, Javadi E, Kadkhodaee M, Sanati A. Enhanced susceptibility to oxidation and diminished vitamin E content of LDL from patients with stable coronary artery disease. Clin Chem 2001;47:1234-40.
[23]. Bremner I. Manifestation of copper excess. . Am J Clin Nutr 1998;67:1069S-73S.
[24]. Kadiiska MB, Hanna PM, Jordan SJ, Mason RP. Electron spin resonance evidence for free radical generation in copper-treated vitamin E- and selenium-deficient rats:in vivo spin-trapping investigation. Mol Pharmacol. 1993;44:222-27.
[25]. Powell SR. The antioxidant properties of zinc. J Nutr 2000;130:1447S-54S.
[26]. Kawanishi S, Inoue S, Yamamoto K. Hydroxyl radical and singlet oxygene production and DNA damage induced by carcinogenic metal compouds and hydrogen peroxide. Biol Trace Elem Res 1989;21:367-72.
[27]. Meryon SD, Jakeman KJ. The effects in vitro of zinc released from dental restorative materials. Int Endod J 1985;18:191-8.
[28]. Panel on micronutrients, Subcommittees on Upper Reference Levels of Nutrients and of Interpretation and Use of Dietary Reference Intakes, Intakes. atSCotSEoDR. Dietary Reference Intakes for Vitamin A, Vitamin K, Arsenic , Boron, Chromium, Copper, Iodine, Iron, Maganese, Molybdenium, Nickel, Silicon, Vanadium and Zinc. In: Press NA, editor. Washington D.C.: National Academy of Sciences; 2000.
[29]. Schuster G, Reichle R, Bauer RR, Schopf PM. Allergies induced by orthodontic alloys: incidence and impact on treatment. Results of a survey in private orthodontic offices in the Federal State of Hesse, Germany. J Orofac Orthop 2004;65:48-59.
[30]. Bishara SE. Oral lesions caused by an orthodontic retainer: a case report. Am J Orthod Dentofacial Orthop 1995;108:115-7.
[31]. . ISO 14577-1 Metallic materials-Instrumented indentation test for hardness and materials parameters: International Organization for Standardization Geneva; 2002.
[32]. ISO10271. Dental metallic materials-Corrosion test methods. Switzerland: International Organisation for Standardization (ISO); 2011.
[33]. Okamoto H. Ag-Ga (Silver-Gallium). Journal of phase Equilibria and Diffusion 2008;29:111.
[34]. Moser Z., Gasior W., Pstrus J., Zakulski W., Ohnuma I., Liu X.J., et al. Studies of the Ag-In phase diagram and surface tension measurements. Journal of Electronic Materials 2001;30:1120-28.
[35]. Jakobson D.M., Sangha S.P.S. Novel application of diffusion soldering. Soldering & Surface mount technology 1996;8:12-15.

[36]. Gupta M. The Ga-Sn-Ni (Gallium-Nickel-Tin) system. Journal of phase Equilibria and Diffusion 2008;29:374-77.
[37]. Zhongmin L., Songbai X., Xianpeng H., Liyong G., Wenhua G. Study on Microstructure and Property of Brazed Joint of AgCuZn-X(Ga, Sn, In, Ni) Brazing Alloy. Rare Metal Materials and Engineering 2010;39:397-400.
[38]. Gunnaes E., Karlsen O.B., Olsen A., Zagierski O.T. Phase relations and crystal structures in the Ag-Ga system. J. Alloys. Compd. 2000;297:144-55.
[39]. Chang Y.A., Goldberg D., Neumann J.P. Phase diagrams and Thermodynamic properties of Ternary Copper-Silver Systems. Journal of Physical Chemistry Referenc Data 1997;6:621-73.
[40]. Vahed A., Lachman N., Knutsen R.D. Failure investigation of soldered stainless steel orthodontic appliances exposed to artificial saliva. Dental Materials 2007;23:855-61.
[41]. Feng J., Zhang L. Interface structure and mechanical properties of the brazed join of TiC cermet and steel. Journal of the European Ceramic Society 2006;26:1287-92.
[42]. Huijie L., Jicai F. Vacuum brazing TiAl-based alloy to 40Cr steel using Ag-Cu-Zn filler metal. Journal of Materials Science Letters 2002;21:9-10.
[43]. Warinsiriruk E., Phung-on I. Microstructure of Induction Brazed Interface between Cobalt-based Alloy and Martensitic Stainless Steel using Ag-Cu-Zn filler metal. Asian International Journal of Science and Technology in Production and Manufacturing Engineering. 2010;3:41-44.
[44]. Zhang L., Feng J., Zhang B., Jing X. Ag-Cu-Zn alloy for brazing TiC cermet/steel. Materials Letters 2005;59:110-13.
[45]. Ardashnikova E.I., Eliseev A.A., Sokolov V.I., Chekmareva P.P. Effect of microstructure on the mechanical properties of cast silver solders. Khimicheskoe i Neftyanoe Mashinostroenie 1978;8:29-30.
[46]. Yoo Y.C., Kim J.H., Park K. Microstructural characterization of Al2O3 /AISI 8650 steel joint brazed with Ag-Cu-Sn-Zr alloy. Materials Letters 2000;42:362-66.
[47]. Karakaya I., Thompson W.T. The Ag-Sn System. Bulletin of Alloy Phase Diagrams. 1987;8:340-41.
[48]. Gierlotka W., Handzlik D. J. Thermodynamic description of the binary Ag-Ga system. J. Alloys. Compd. 2011;509:38-42.
[49]. Weise W, Voelcker A, Kaufmann D, Malikowski W, Beuers J, Krappitz H, inventors. Use of a Cadmium-Free Silver Alloy as Brazing Solder (III) USP 5341981. US patent 5341981. Aug. 30, 1994.
[50]. Weise W MW, Kaufmann D, Krappitz H, inventor. Cadmium-Free Silver Alloy as Low Melting Brazing Filler Material. USP6299835. Oct. 9, 2001.
[51]. Johnston WM, Kao EC. Assessment of appearance match by visual observation and clinical colorimetry. J Dent Res 1989;68:819-22.
[52]. Faverjon F, Hopkinson A, Storey J, inventors. Silver Alloy Compositions. . Jul.10, 2008.

Figure Captions

Figure 1: DSC thermograms for AgGa(A), AgGaSn(B), AgIn(C) and AgSn(D) experimental alloys.

Figure 2. BEI images of DEN (A), LEO (B), NOB(C) and ORT (D), AgGa(E), AgGaSn(F), AgIn(G) and AgSn(H) at 1000X nominal magnification. Inset in LEO represents a 3000X nominal magnification image. The locations where spot analysis was performed are noted with asterisks and characterized as L (low mean atomic number), M (medium mean atomic number) and H (High mean atomic number).

Figure 3: XRD spectra of materials tested. Although the spectra were acquired from 30 to 110 degrees only the range 35 ~70^{o} is presented here for the sake of clarity (only minor peaks were identified at higher angles).
1: Ag rich (FCC) solid solution
2: Cu rich (FCC) solid solution
3: BCC β phase
4: Ag_3Ga (hexagonal)
5: AgIn (cubic)

(FCC: face centered cube, BCC: body centered cube)

Figure 4: Representative force-indentation depth curves for all materials tested.

Figure 5: Mean values and standard deviations of ion release per unit surface for Cu, Zn and Ga in Ringer's solution. Standard deviations are tiny and hardly shown in most cases.

Figure 6: Mean values and standard deviations of ion release per unit surface for Cu, Zn and Ga in NaCl solution. Standard deviations are tiny and hardly shown in most cases.

Figure 7: Representative optical microscopy images of commercial (A) and experimental (B) alloys tested. A higher magnification image with dendritic structure is appeared in inset in B.

Figure 8: DE values in descending order. Horizontal lines connect mean values without statistical significant differences ($p>0.05$).

Table 1: Brand name, composition and melting temperature range of the commercial alloys tested according to manufacturers as well as the composition of the experimental alloys.

Material	Composition (wt.%)	Melting range (^{o}C)	Code
Dentaurum	Ag:59, Cu:16, Zn:25	655-680	DEN
Leone	Ag:55, Cu:21, Zn:22, Sn:2	630-660	LEO
Nobil	Ag:59, Cu:16, Zn:25	655-680	NOB
Ortho	Ag:1.5-55, Cu:19-95,Zn:2-44, Ni:0.1-24	660*	ORT
AgGa	Ag:88, Ga:12		AgGa
AgGaSn	Ag:85,Ga:10, Sn:5		AgGaSn
AgIn	Ag:80,In:20		AgIn
AgSn	Ag:93, Sn:7		AgSn

[1] Dentaurum Universal silver solder (Dentaurum, Ispringen, Germany)
[2] Leone R0224-00 (Leone Florence. Italy)
[3] Nobil Metal Solder LV15 (Nobil Metal, Villa Franca d'Asti, Italy)
[4] Ortho Technology silver solder #2020 (Ortho Technology Inc. Tampa, FL)
* Only solidus temperature is provided.

Table 2: Elemental composition (wt%) of all materials and constituent phases based on mean atomic number contrast of BEI after EDX analysis. The results of L, M and H have been acquired by spot analysis. Only the average value of each element is shown.

Alloy		Ag	Zn	Cu	Ga	Sn	In	Ni
Den	Area	61.7	22.7	15.3				
	L	57.2	22.5	20.6				
	H	70.4	18.5	10.9				
Leo	Area	49.5	24.7	23.6		1.8		
	L	11.0	32.9	51.7		4.2		
	M	53.1	22.0	22.9		2.0		
	H	59.0	23.7	14.0		3.5		
Nob	Area	61.0	22.3	16.6				
	L	60.7	21.1	18.4				
	H	69.6	19.3	11.1				
Ort	Area	48.7	26.8	21.3				3.2
	L	10.1	34.9	42.3				12.7
	M	52.8	24.0	21.6				1.4
	H	60.2	23.1	15.0				1.8
AgGa	Area	88.7			11.2			
	L	81.7			18.3			
	H	90.4			9.6			
AgGaSn	Area	85.9			9.3	5.2		
	L	78.2			13.5	8.4		
	H	86.3			6.9	6.6		
AgIn	Area	81.2					18.9	
AgSn	Area	92.7				7.2		

Table 3. Mean values and standard deviations in parentheses of Martens hardness (HM), indentation modulus (E_{IT}) and elastic index (η_{IT}) for all materials tested.

Alloy	HM (N/mm^2)	E_{IT} (GPa)	n_{IT} (%)
DEN	1140(72)[1]	44.4(2.8)[1]	21.3(2.0)[1]
LEO	1127(151)[1]	55.0(5.8)[2]	22.5(2.4)[2]
NOB	1039(65)[1]	39.5(3.2)[1]	26.1(2.6)[1]
ORT	1173(26)[1]	60.5(1.9)[2]	16.6(0.6)[3]
AgGa	624(130)[2]	41.1(3.2)[3]	15.9(2.9)[3,4]
AgGaSn	492(65)[2,3]	36.7(3.9)[3]	13.7(1.0)[4]
AgIn	407(34)[3,4]	42.0(4.7)[3]	13.6(1.0)[4]
AgSn	380(28)[4]	42.2(3.7)[3]	9.6(0.7)[5]

Same superscript indicate mean values without statistical significant difference ($p>0.05$)

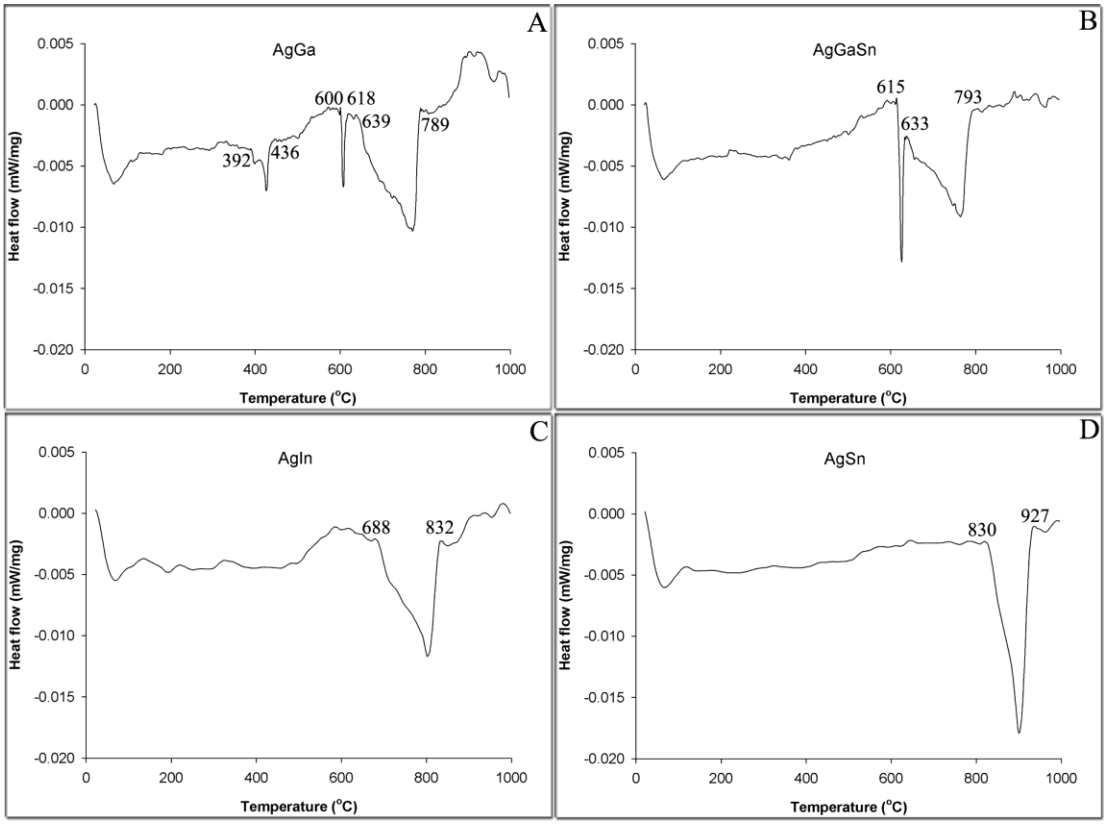
A
AgGa
392
436
600
618
639
789
B
AgGaSn
615
633
793
C
AgIn
688
832
D
AgSn
830
927
Heat flow (mW/mg)
Temperature (°C)
0.005
0.000
-0.005
-0.010
-0.015
-0.020
0
200
400
600
800
1000

FIG 1.

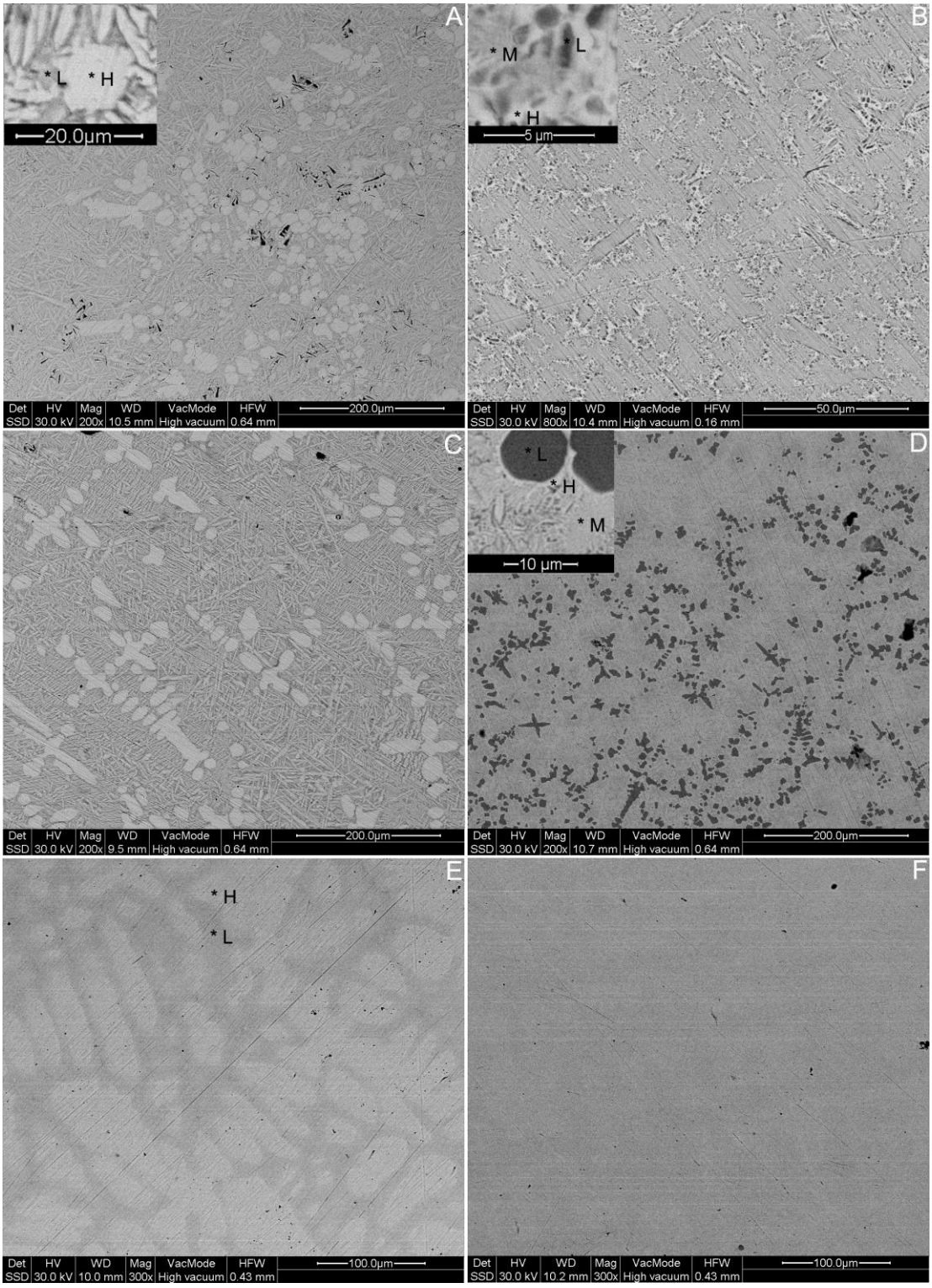
A
*L
*H
20.0µm
Det SSD
HV 30.0 kV
Mag 200x
WD 10.5 mm
VacMode High vacuum
HFW 0.64 mm
200.0µm
B
*M
*L
*H
5 µm
Det SSD
HV 30.0 kV
Mag 800x
WD 10.4 mm
VacMode High vacuum
HFW 0.16 mm
50.0µm
C
Det SSD
HV 30.0 kV
Mag 200x
WD 9.5 mm
VacMode High vacuum
HFW 0.64 mm
200.0µm
D
*L
*H
*M
10 µm
Det SSD
HV 30.0 kV
Mag 200x
WD 10.7 mm
VacMode High vacuum
HFW 0.64 mm
200.0µm
E
*H
*L
Det SSD
HV 30.0 kV
WD 10.0 mm
Mag 300x
VacMode High vacuum
HFW 0.43 mm
100.0µm
F
Det SSD
HV 30.0 kV
WD 10.2 mm
Mag 300x
VacMode High vacuum
HFW 0.43 mm
100.0µm

Fig 2

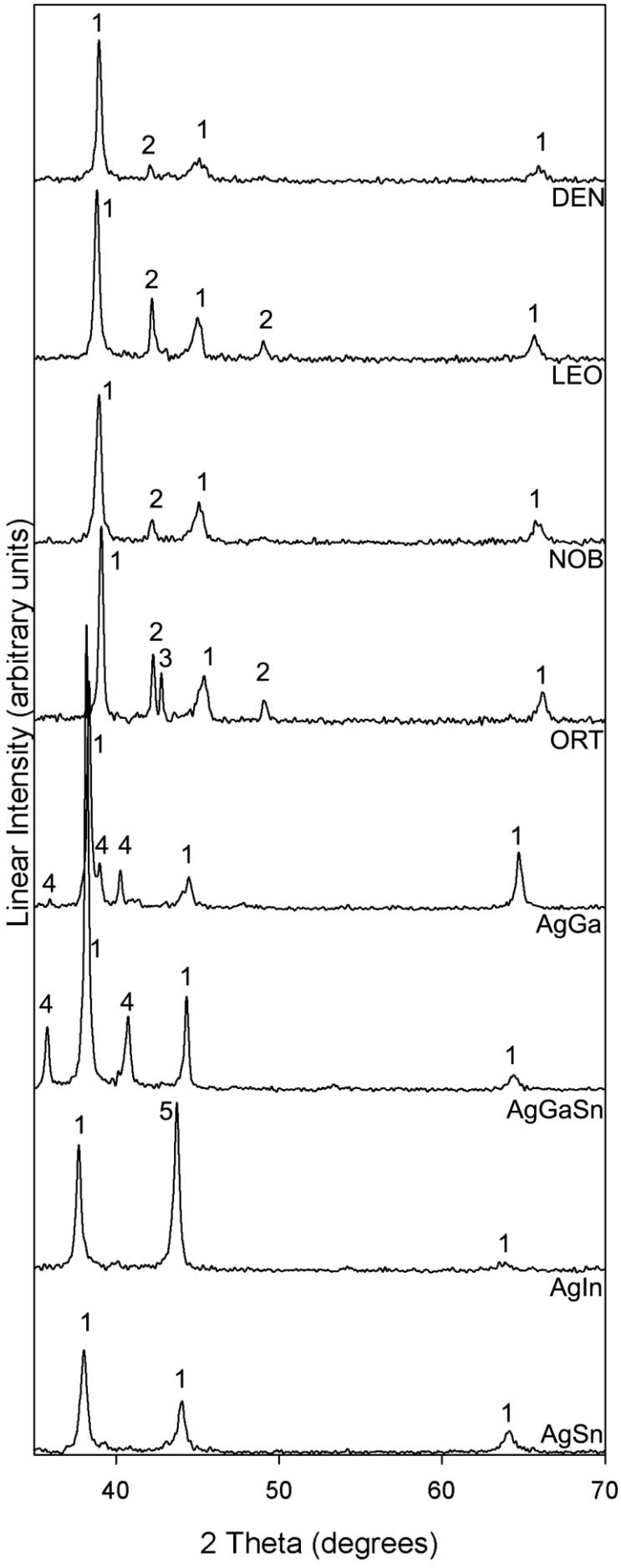
Linear Intensity (arbitrary units)
2 Theta (degrees)
40
50
60
70
DEN
LEO
NOB
ORT
AgGa
AgGaSn
AgIn
AgSn

Fig 3

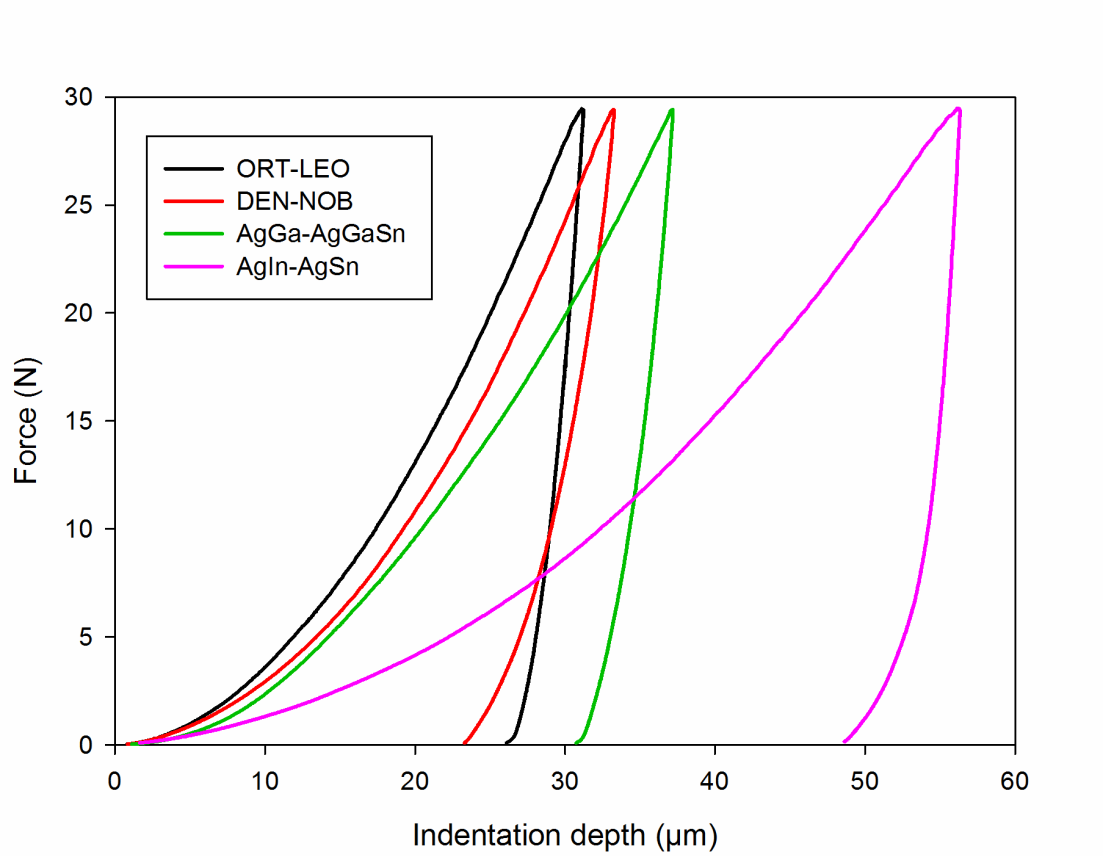
ORT-LEO
DEN-NOB
AgGa-AgGaSn
AgIn-AgSn
Force (N)
Indentation depth (μm)
0
5
10
15
20
25
30
0
10
20
30
40
50
60

Fig 4

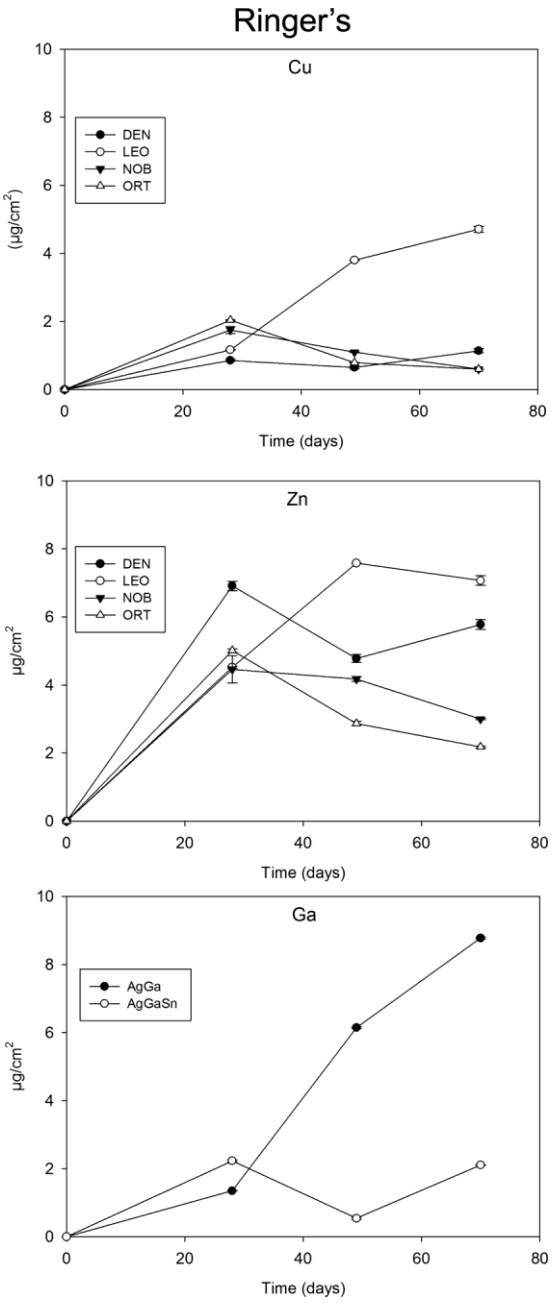
Ringer's
Cu
DEN
LEO
NOB
ORT
(µg/cm²)
Time (days)
Zn
DEN
LEO
NOB
ORT
µg/cm²
Time (days)
Ga
AgGa
AgGaSn
µg/cm²
Time (days)

Fig 5

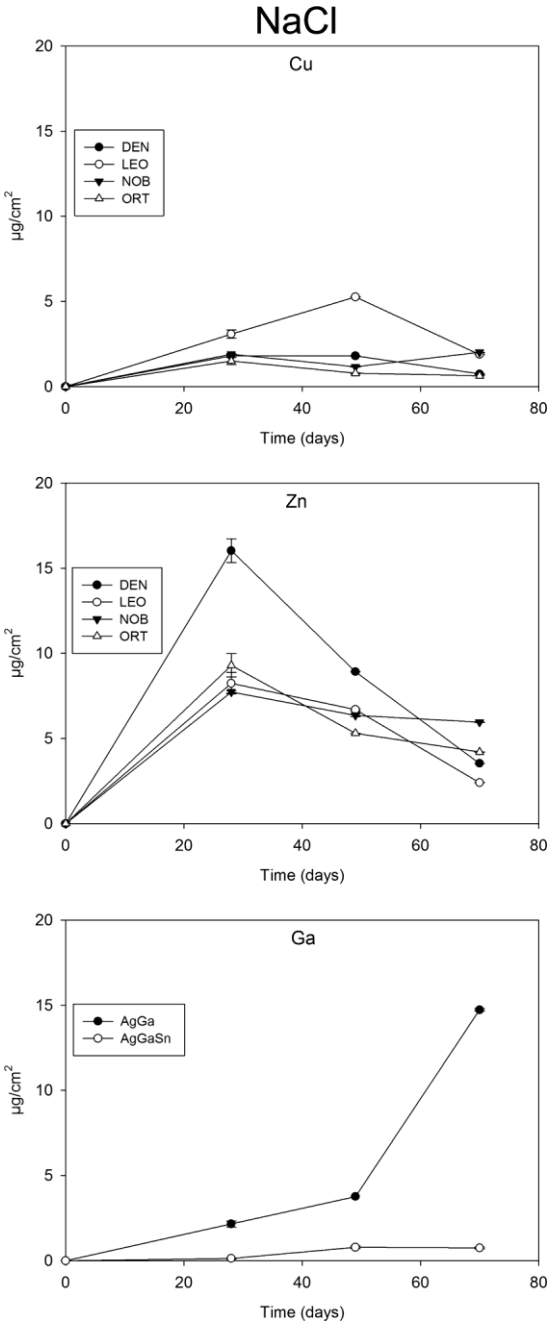
NaCl
Cu
DEN
LEO
NOB
ORT
µg/cm2
Time (days)
Zn
DEN
LEO
NOB
ORT
µg/cm2
Time (days)
Ga
AgGa
AgGaSn
µg/cm2
Time (days)

Fig 6

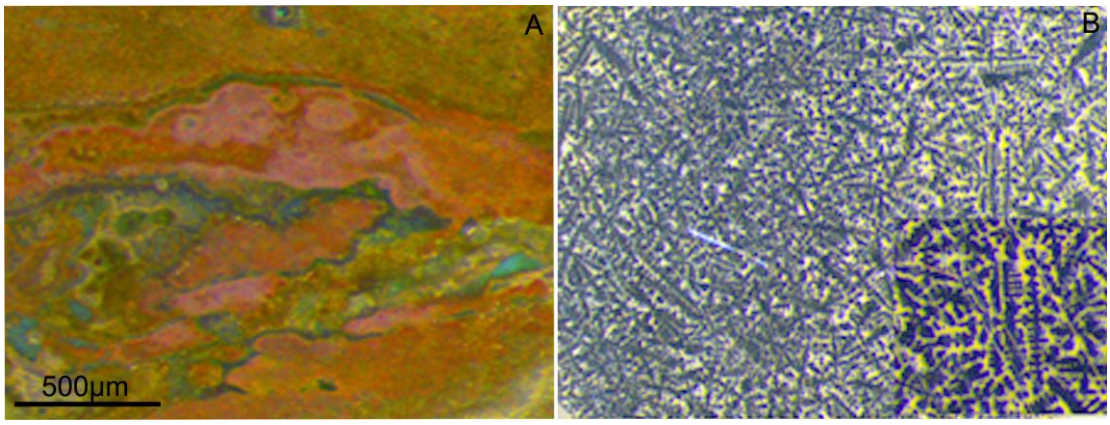
A
500µm
B

Fig 7

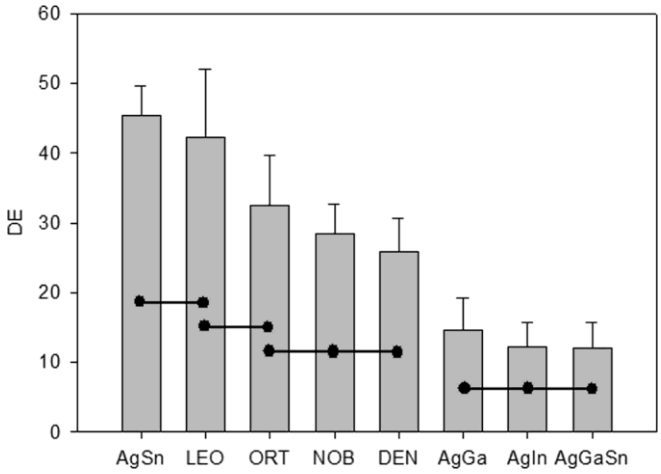

Fig 8